Hindawi
International Journal of Antennas and Propagation
Volume 2019, Article ID 4656141, 7 pages
https://doi.org/10.1155/2019/4656141

Research Article

A Wideband Differential-Fed Microstrip Patch Antenna Based on Radiation of Three Resonant Modes

Taohua Chen, Yueyun Chen, and Rongling Jian

University of Science & Technology Beijing, College Road 30, Haidian District, Beijing, China

Correspondence should be addressed to Yueyun Chen; chenyy@ustb.edu.cn

Received 1 May 2019; Accepted 18 June 2019; Published 28 August 2019

Academic Editor: Eva Antonino-Daviu

A wideband differential-fed microstrip patch antenna based on radiation of three resonant modes of TM_{12}, TM_{30}, and slot is proposed in this paper. Firstly, two symmetrical rectangular slots are cut on the radiating patch where the zero-current position of the TM_{30} mode excites another resonant slot mode. In addition, the slot's length is enlarged to decrease the frequency of the slot mode with little effect on that of the TM_{30} mode. To further expand the impedance bandwidth, the width of patch is reduced to increase the frequency of the TM_{12} mode, while having little influence on that of the TM_{30} and slot modes. Moreover, a pair of small rectangular strips is adopted on the top of the feeding probes to achieve a good impedance matching. Finally, based on the arrangements above, a broadband microstrip patch antenna with three in-band minima is realized. The results show that the impedance bandwidth ($|S_{dd11}| < -10$ dB) of the proposed antenna is extended to 35.8% at the profile of 0.067 free-space wavelength. Meanwhile, the proposed antenna maintains a stable radiation pattern in the operating band.

1. Introduction

Microstrip patch antennas (MPAs) have been extensively investigated and developed over the past decades because of their advantages of low profile, small cost, ease of manufacture, and so on [1]. However, conventional MPAs always suffer from a narrow impedance bandwidth of about 3% because of the high-quality factor Q [2]. In order to expand the impedance bandwidth, a few approaches have been proposed in past decades.

The simplest method to expand the bandwidth is to enhance the antenna thickness and decrease the substrate permittivity, which can reduce the quality factor Q [3]. However, thick substrates enlarge the surface wave leakage leading to poor radiation efficiency, and decreasing the permittivity is limited because the lowest substrate dielectric constant is 1. In addition, the feeding scheme was reconfigured in [4] to extend the impedance bandwidth to 115% at the profile of 0.25 λ_0 (λ_0 is the free-space wavelength); the reason for bandwidth enhancement is that another nonradiative resonant mode is introduced around the fundamental mode. However, it is difficult to implement the feeding scheme in a thin substrate. Moreover, the authors in [5] used a Wang-shaped radiating patch to extend the bandwidth of 49.3% with the profile of 0.2 λ_0. In [6], an inverted U-shaped slot was adopted on the radiating patch to extend the impedance bandwidth to 17.8% with the thickness of 0.09 λ_0. In [7], a simple E-shaped patch was proposed for bandwidth enhancement, and the impedance bandwidth was expanded to 30.3% at the 0.1 λ_0 profile. Nevertheless, all the antennas mentioned above always need a high profile, which will destroy the low-profile property of microstrip antenna.

Furthermore, in recent years, coupling two odd modes of MPAs together becomes a new attractive method because of keeping the advantage of low profile of MPAs. In [8], the TM_{10} and TM_{30} modes were combined to extend the bandwidth to 18% at the height of 0.08 λ_0. In [9], the authors proposed to combine TM_{10} and TM_{12} modes together, and the impedance bandwidth was enlarged to 10% with the profile of 0.039 λ_0. Additionally, The TM_{12} and TM_{30} modes were also adopted to achieve bandwidth enhancement in [10], and a bandwidth of 14.8% was realized at the profile of 0.048 λ_0. However, since only two odd modes are combined,

the impedance bandwidth of these antennas is only twice as wide as that of traditional microstrip antennas, which may hinder the application of these MPAs in broadband communication systems.

In this paper, a novel wideband differential-fed MPA based on radiation of three resonant modes of TM_{12}, TM_{30}, and slot is proposed. Firstly, two symmetrical rectangular slots are cut at the position of zero-current of the TM_{30} mode of the radiating patch to excite another resonant slot mode with little effect on the TM_{30} mode. Besides, through increasing the slot's length, the TM_{30} and slot modes can be adjusted in proximity to each other. To further expand the impedance bandwidth, the patch width is reduced to increase the frequency of the TM_{12} mode. With these arrangements, the TM_{12}, TM_{30}, and slot modes can be combined to form a wideband. Moreover, a pair of small rectangular strips is used on the top of the feeding probes to achieve a good impedance matching. The results show that the proposed antenna has realized an impedance bandwidth ($|S_{dd11}| < -10$ dB) of 35.8% at the profile of 0.067 λ_0. Additionally, the proposed antenna maintains a stable radiation pattern over the operating band.

2. Geometry and Design Process

The geometry of the proposed differential-fed wideband MPA is shown in Figure 1. It consists of a radiating patch with the size of $L \times W$ and a ground plane with the size of $L_S \times W_S$. And a dielectric substrate RO5880 with permittivity of $\varepsilon_r = 2.2$ and thickness of $H_1 = 0.508$ mm is selected in this paper for antenna design. The radiating patch is printed on the top surface of the substrate RO5880, while the ground plane is placed below the substrate with an air gap of $H = 3$ mm. Meanwhile, two symmetrical rectangular slots ($L_1 \times W_1$) with the spacing of D_1 are cut on the radiating patch, which can excite another resonant slot mode. In addition, differential-fed with spacing of D_2 is used and a pair of small rectangular strips ($L_2 \times W_2$) is adopted on the top of the feeding probes. All parameters for the proposed antenna in Figure 1 are tabulated in Table 1. In this paper, HFSS 13.0 is used for simulation calculation.

Firstly, as can be seen from Figure 2(a), a square MPA with differential-fed scheme is used for antenna design to suppress the undesired even-order modes which are null in the boresight [11]. Secondly, in Figure 2(b), two symmetrical rectangular slots are cut on the radiating patch to excite another slot mode near the TM_{30} mode to expand the bandwidth. Thirdly, to further enlarge the bandwidth, in Figure 2(c), the patch width is reduced to increase the frequency of the TM_{12} mode to proximity to that of the slot and TM_{30} modes. Finally, in Figure 2(d), the slot's width and position are modified slightly and a pair of small rectangular strips is adopted on the top of the feeding probes to achieve a good impedance matching.

3. Parametric Studies and Design Flow

3.1. Exciting Another Resonant Slot Mode. The current distribution of the TM_{30} mode of the patch is plotted in Figure 3. It can be seen from Figure 3 that there are two zero-current lines on the patch. Therefore, as shown in Figure 2(b), when slots are cut on the patch near these positions, it will have little effect on the TM_{30} mode while can excite the resonant slot mode. Through modifying the slot's length properly, TM_{30} and slot modes can be combined to expand the bandwidth. To better understand the effect of slot length, the frequency of the TM_{30} mode (f_{30}) and slot mode (f_{slot}) under different slot length L_1 is plotted in Figure 4. Note that, in this subsection, the W_1 is 1 mm and D_1 is 21 mm.

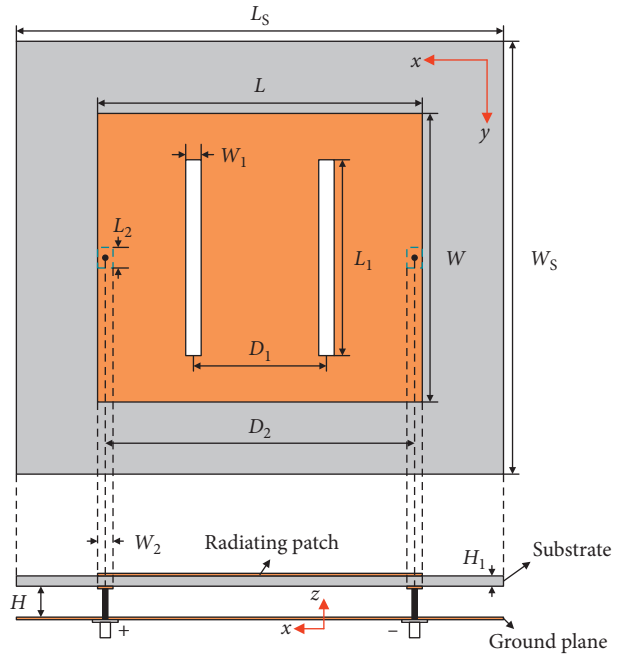

Figure 1: Geometry of the proposed wideband antenna.

It can be observed from Figure 4 that when slot length increases from 18 to 38 mm, the f_{slot} decreases from 7.2 GHz to 5.1 GHz clearly while f_{30} keeps constant at 6.24 GHz. Considering the whole performance, in this paper, $L_1 = 38$ mm is selected for the widest bandwidth.

3.2. Increasing the Frequency of TM_{12} Mode. To further extend the bandwidth, the TM_{12} mode is adjusted in proximity to slot and TM_{30} modes in this paper. According to the cavity model [12], the resonant frequencies (f_{mn}) of TM_{mn} modes in MPA can be expressed as follows:

$$f_{mn} = \frac{c}{2\sqrt{\varepsilon_r}} \times \sqrt{\left(\frac{m}{L}\right)^2 + \left(\frac{n}{W}\right)^2}, \quad (1)$$

where c is the light speed in the free space, ε_r is the dielectric constant of substrate, and $m = 1, 2, 3, \ldots$, and $n = 1, 2, 3, \ldots$

Based on formula (1), the patch width (W) plays an important role in the frequency of TM_{12} mode (f_{12}), yet has little effect on f_{30}. And the f_{slot} is mainly decided on the slot length, so the patch width also has little effect on f_{slot}. Therefore, when W is reduced, f_{12} will be increased

Table 1: Dimensions of the proposed antenna.

Parameters	L	L_S	L_1	L_2	W	W_S	W_1	W_2	D_1	D_2	H	H_1
Values (mm)	63	94.5	38	4	56	84	3	3	25.8	60	3	0.508

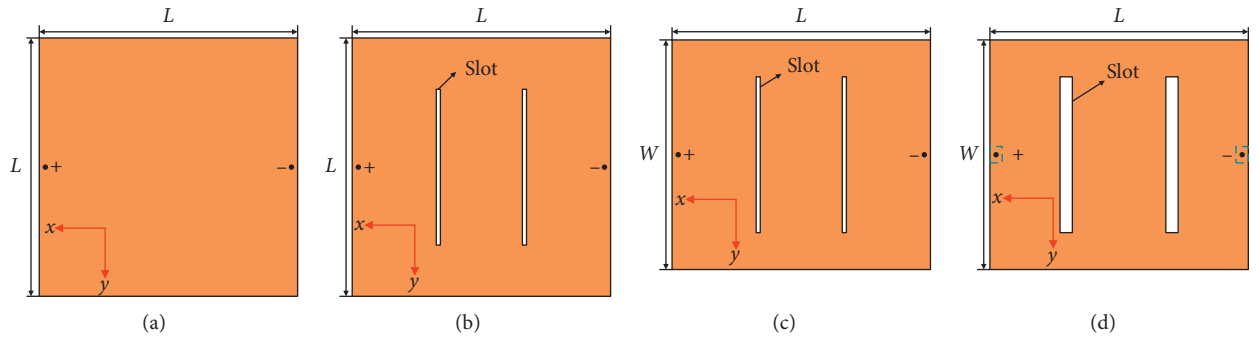

Figure 2: Design process of proposed wideband antenna. (a) Conventional MPA. (b) MPA with two slots. (c) MPA with two slots and shortened patch. (d) MPA with two slots, shortened patch and a pair of strips.

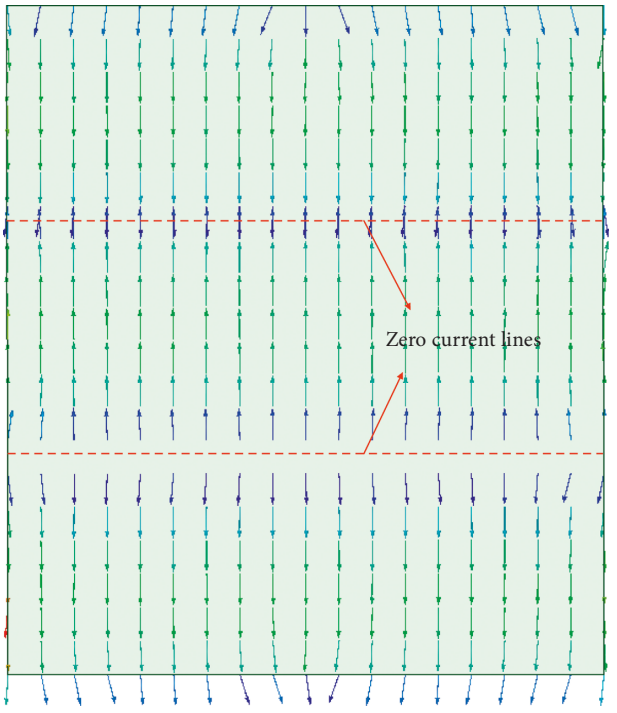

Figure 3: Current distribution of TM_{30} mode.

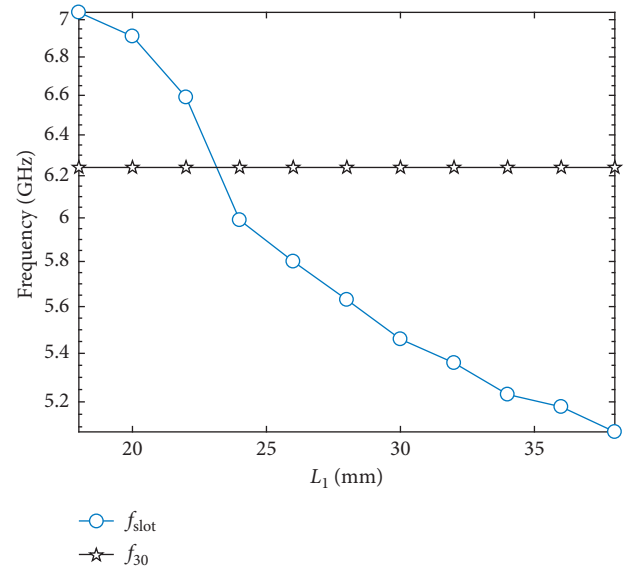

Figure 4: f_{30} and f_{slot} at different slots length L_1.

while f_{30} and f_{slot} keep constant. To better understand how the patch width influences f_{12}, f_{30}, and f_{slot}, Figure 5 plots f_{12}, f_{30}, and f_{slot} varying with patch width W. W_1, D_1, and L_1 are selected as 1 mm, 21 mm, and 38 mm, respectively.

We can see from Figure 5 that when W reduces from 63 to 56 mm, f_{12} increases from 4.18 GHz to 4.44 GHz while f_{30} and f_{slot} keep constant, which is consistent with the analysis above. Note that when $W = 56$ mm, the spacing of TM_{12} and slot modes is enough to form the wideband. Therefore, in this paper, we choose $W = 56$ mm for antenna design.

3.3. Impedance Matching. With the arrangements above, the TM_{12}, TM_{30}, and slot modes have been in proximity to each other. However, the input impedance is mismatch. To finally obtain a wideband MPA, the slot position (D_1) and width (W_1) are modified and a pair of small rectangular strips is adopted on the top of the feeding probes to achieve a good impedance matching. In this subsection, we analyze the effects of slots and rectangular strips on impedance matching. When one parameter is studied, the other parameters are fixed as listed in Table 1.

Figure 6 illustrates $|S_{dd11}|$ as a function of frequency at different slot position D_1. As can be seen from Figure 6, the slot position has great effects on impedance matching and bandwidth. Proper design of the slots position can achieve a better impedance matching and wider bandwidth. In this

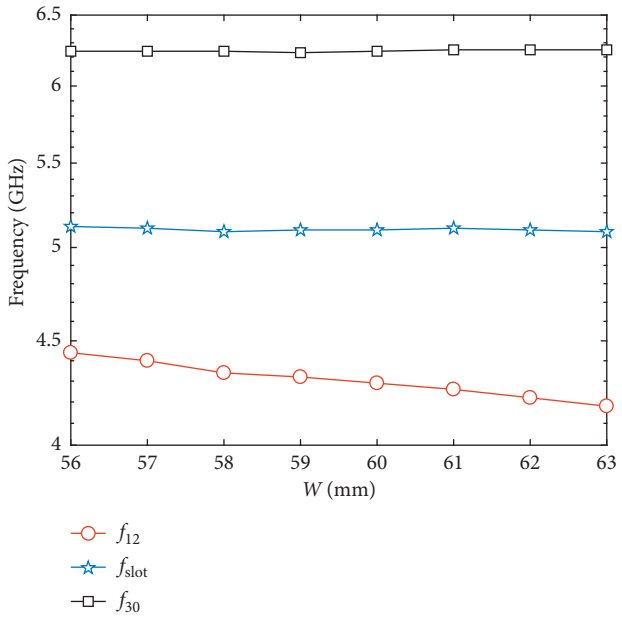

Figure 5: f_{12}, f_{30} and f_{slot} varies with patch width W.

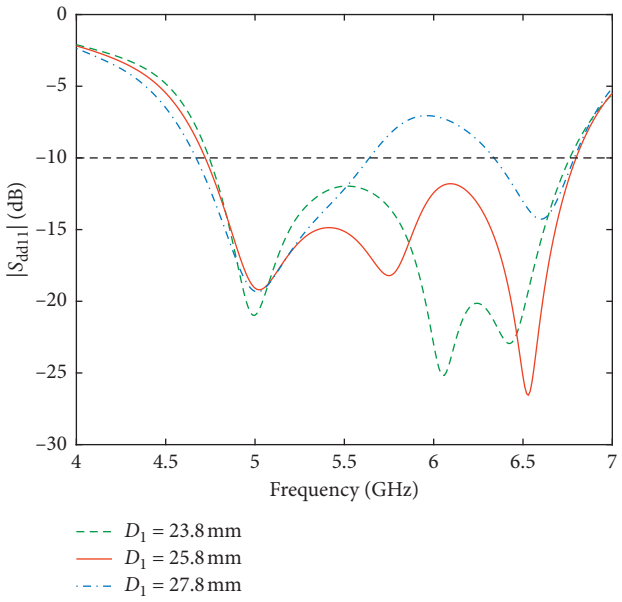

Figure 6: $|S_{dd11}|$ as a function of frequency at different slots position D_1.

paper, considering the whole $|S_{dd11}|$ performance in Figure 6, the $D_1 = 25.8$ mm is selected for antenna design.

Figure 7 shows $|S_{dd11}|$ as a function of frequency at different slot width W_1. Like slots position D_1, the slots width W_1 also has large influences on impedance matching and bandwidth. Compare the whole $|S_{dd11}|$ performance at different slot width W_1, the best bandwidth is achieved at $W_1 = 3$ mm.

Besides, in this paper, a pair of small rectangular strips is adopted on the top of the feeding probes to eliminate the inductance introduced by probes for good impedance

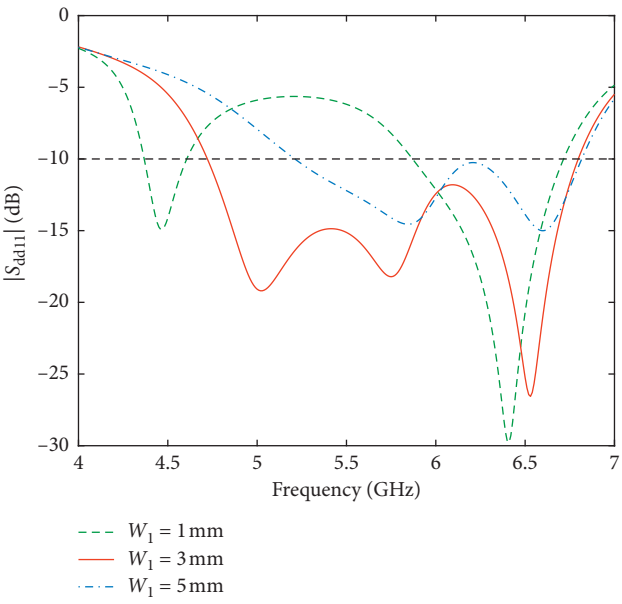

Figure 7: $|S_{dd11}|$ as a function of frequency at different slots width W_1.

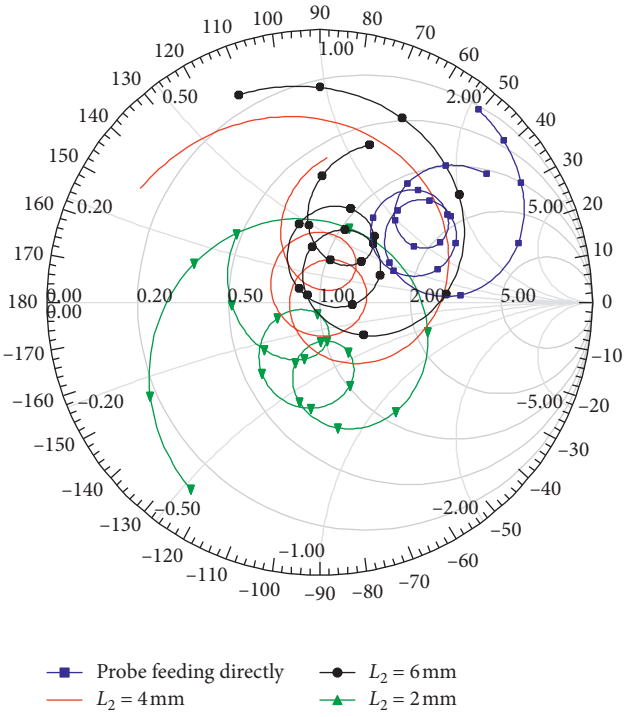

Figure 8: Smith chart of proposed wideband MPA at different L_2.

matching. Note that the value of capacitance introduced by the rectangular strips is mainly decided with the area of these rectangular strips. Therefore, we only modify the strips length L_2 to achieve impedance matching and keep W_2 as listed in Table 1. Figure 8 plots the Smith chart of proposed wideband MPA at different L_2.

From Figure 8, we can find that the input impedance is inductive as the probes connect radiating patch directly.

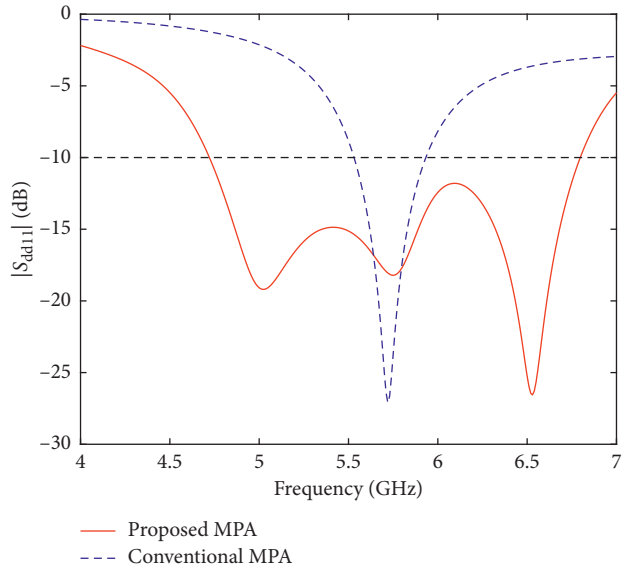

Figure 9: Reflection coefficient of proposed wideband MPA and conventional MPA.

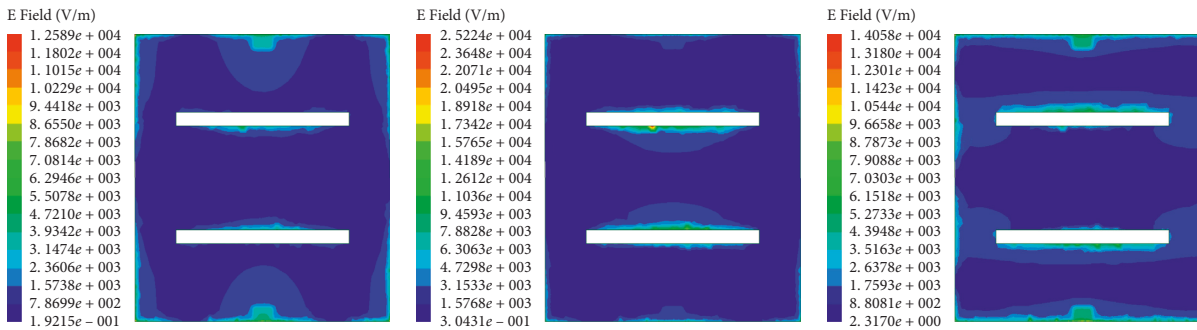

Figure 10: Electric field distributions underneath the radiating patch of proposed wideband MPA. (a) 5.02 GHz. (b) 5.75 GHz. (c) 6.53 GHz.

When a pair of rectangular strips is adopted on the top of the probes to capacitive-coupled feed and L_2 decreases from 6 mm to 2 mm, the input impedance gradually changes from inductive to capacitive. It can also be observed from Figure 8 that the best L_2 is 4 mm.

4. Results and Discussion

The reflection coefficient of proposed wideband MPA is plotted in Figure 9. It can be observed that the impedance bandwidth for $|S_{dd11}| < -10$ dB is 35.8%, covering from 4.72 to 6.79 GHz. Besides, there are three minima over the operating band, which is consistent with the three resonant modes mentioned above. Meanwhile, the reflection coefficient of conventional MPA at the same profile is also plotted in Figure 9. Compared with the traditional MPA, the impedance bandwidth of the proposed antenna has enhanced to more than three times, which indicates that the proposed antenna can extend the bandwidth distinctly.

Figure 10 plots the electric field distributions underneath the radiating patch at three minima of 5.02, 5.75, and 6.53 GHz. For the first minimum at 5.02 GHz, it can be found from Figure 10(a) that there are two vertical zero electric field lines and one horizontal zero electric field line, which is same as the electric field distributions of the TM_{12} mode of a conventional patch antenna. Thus, it is TM_{12} mode that works at 5.02 GHz. As for the second minimum at 5.75 GHz, the electric field is mainly distributed around two slots and is rarely around the radiative and nonradiative edges of the traditional microstrip antenna, which can be observed from Figure 10(b). This shows that the slot mode works at 5.75 GHz. While for the third minimum at 6.53 GHz, it can be clearly seen from the Figure 10(c) that there are three horizontal zero electric field lines, which indicates the proposed MPA resonates at the TM_{30} mode.

Figure 11 gives the normalized radiation patterns of the proposed wideband MPA at three minima of 5.02, 5.75, and 6.53 GHz. The copolarization radiation patterns are symmetric in both E-plane and H-plane and have the peaks in the broadside direction, which shows that the proposed wideband MPA maintains a stable radiation pattern over the operating band. Meanwhile, a good cross-polarization characteristic of lower than −25 dB is achieved.

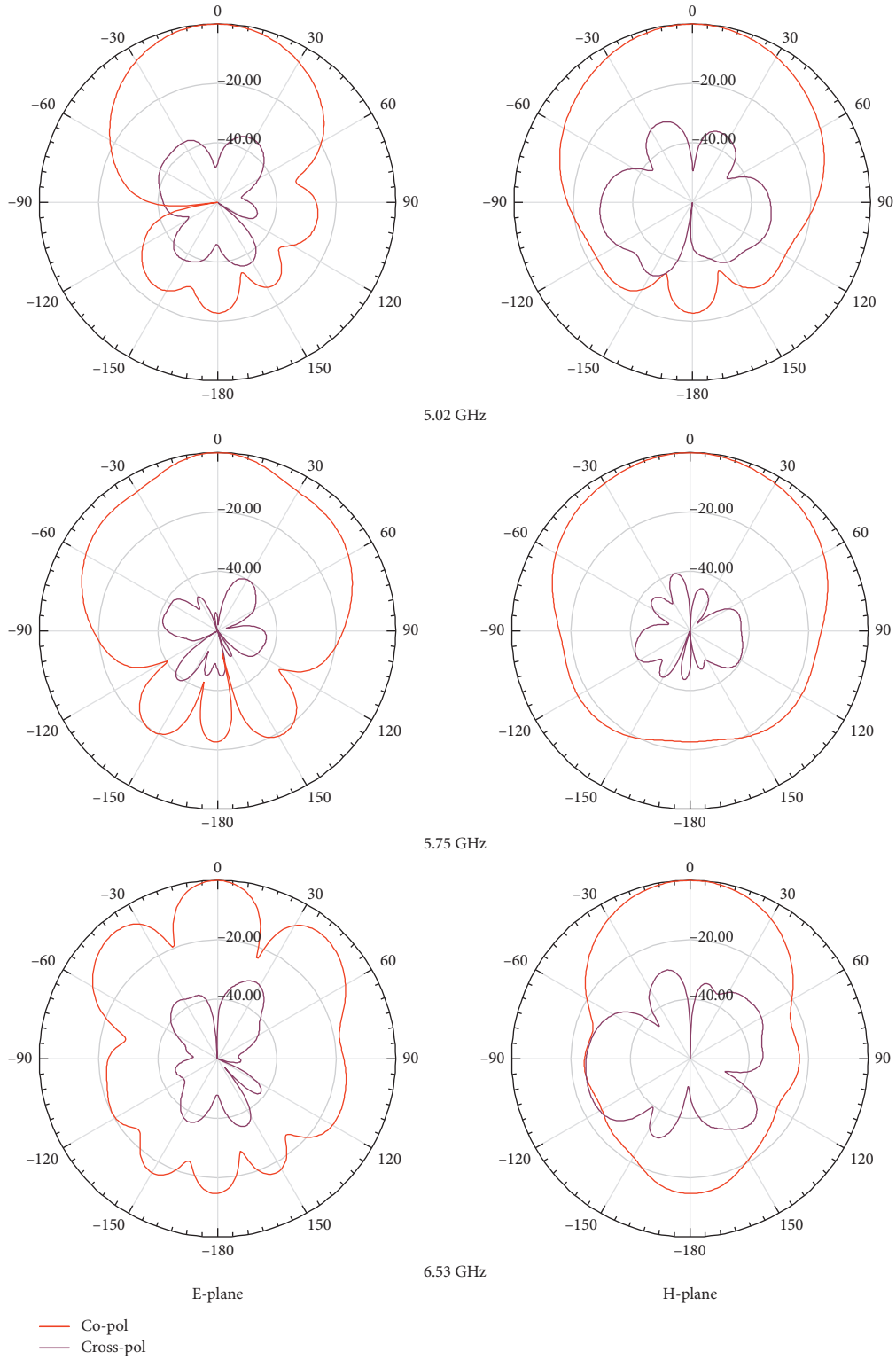

Figure 11: Normalized radiation patterns of proposed wideband MPA.

In addition, the gain, directivity, and efficiency as functions of frequency at broadside direction of the proposed antenna are illustrated in Figure 12. Over the operating band, the gain ranges from 8.8 to 13.24 dBi and the efficiency is above 90%. It can also be observed from Figure 12 that the gain is dropped at about 5.7-5.8 GHz. The reason is that for the proposed wideband antenna, the slot mode between TM_{12} and TM_{30} modes resonates in this band, and the gain of slot mode is lowest among three resonant modes.

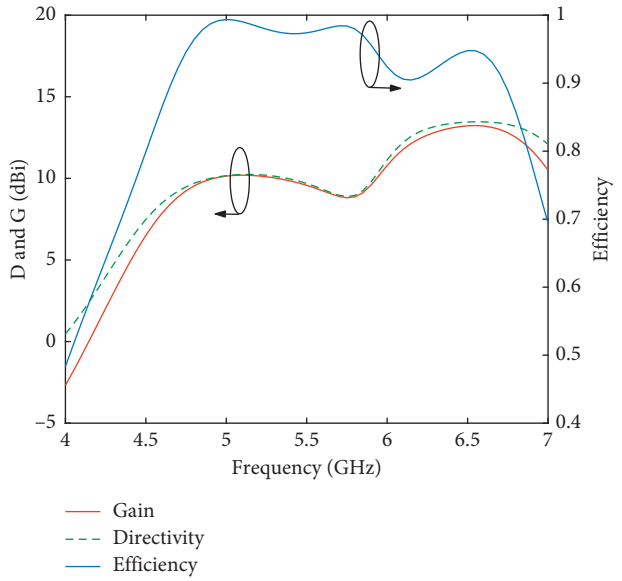

Figure 12: Gain, directivity, and efficiency as functions of frequency at broadside direction of proposed wideband MPA.

5. Conclusion

In this paper, a wideband differential-fed microstrip patch antenna based on radiation of three resonant modes of the TM_{12}, TM_{30}, and slot is proposed and analyzed. First, two symmetrical rectangular slots are cut on the radiating patch, which will excite another resonant slot mode near the TM_{30} mode to extend the impedance bandwidth. Second, to further expand the bandwidth, the width of the patch is reduced to increase the frequency of the TM_{12} mode with little effect on that of TM_{30} and slot modes. Moreover, a good impedance matching is achieved through adopting a pair of small rectangular strips on the top of the feeding probes. Finally, a wideband microstrip patch antenna with an impedance bandwidth of 35.8% is realized under a low profile of 0.067 λ_0. Besides, the proposed antenna maintains a stable radiation pattern and a good efficiency above 90% over the operating band. The proposed antenna is compact and has a wideband, it can be used for modern wireless communication systems.

Data Availability

The data in the HFSS used to support the findings of this study were supplied by Taohua Chen under license and so cannot be made freely available. Requests for access to these data should be made to Taohua Chen, 18813127085@163.com.

Conflicts of Interest

The authors declare that they have no conflicts of interest.

Acknowledgments

This work was supported by the National Science and Technology Major Project of China (no. 2017ZX03001021-005).

References

[1] W. Sun, Y. Li, Z. Zhang, and Z. Feng, "Broadband and low-profile microstrip antenna using strip-slot hybrid structure," *IEEE Antennas and Wireless Propagation Letters*, vol. 16, pp. 3118–3121, 2017.

[2] A. B. Constantine, *Antenna Theory: Analysis and design. Microstrip Antennas*, John Wiley & Sons, Hoboken, NJ, USA, 3rd edition, 2005.

[3] R. Bancroft, *Microstrip and Printed Antenna Design*, The Institution of Engineering and Technology, London, UK, 2009.

[4] S. W. Liao, Q. Xue, and J. H. Xu, "Parallel-plate transmission line and L-plate feeding differentially driven H-slot patch antenna," *IEEE Antennas & Wireless Propagation Letters*, vol. 11, no. 8, pp. 640–644, 2012.

[5] K. L. Chung and C.-H. Wong, "Wang-shaped patch antenna for wireless communications," *IEEE Antennas and Wireless Propagation Letters*, vol. 9, pp. 638–640, 2010.

[6] A. Singh and S. Singh, "Miniaturized wideband aperture coupled microstrip patch antenna by using inverted U-slot," *International Journal of Antennas and Propagation*, vol. 2014, Article ID 306942, 7 pages, 2014.

[7] F. Yang, X.-X. Zhang, X. Ye, and Y. Rahmat-Samii, "Wide-band E-shaped patch antennas for wireless communications," *IEEE Transactions on Antennas and Propagation*, vol. 49, no. 7, pp. 1094–1100, 2001.

[8] D. Wang, K. B. Ng, C. H. Chan, and H. Wong, "A novel wideband differentially-fed higher-order mode millimeter-wave patch antenna," *IEEE Transactions on Antennas and Propagation*, vol. 63, no. 2, pp. 466–473, 2015.

[9] N.-W. Liu, L. Zhu, W.-W. Choi, and X. Zhang, "A low-profile differential-fed patch antenna with bandwidth enhancement and sidelobe reduction under operation of TM10 and TM12 modes," *IEEE Transactions on Antennas and Propagation*, vol. 66, no. 9, pp. 4854–4859, 2018.

[10] N.-W. Liu, L. Zhu, W.-W. Choi, and G. Fu, "A low-profile wideband Aperture-fed microstrip antenna with improved radiation patterns," *IEEE Transactions on Antennas and Propagation*, vol. 67, no. 1, pp. 562–567, 2019.

[11] Y. P. Zhang and J. J. Wang, "Theory and analysis of differentially-driven microstrip antennas," *IEEE Transactions on Antennas and Propagation*, vol. 54, no. 4, pp. 1092–1099, 2006.

[12] R. Garg, P. Bhartia, I. Bahl, and A. Ittipiboon, *Microstrip Antenna Design Handbook*, Artech House, Norwood, Massachusetts, USA, 2001.